Molecular Thermodynamics for Salt-Induced Protein Precipitation

Y. C. Chiew, D. Kuehner, H. W. Blanch, and J. M. Prausnitz
Dept. of Chemical Engineering, University of California, Berkeley, CA 94720
Lawrence Berkeley Laboratory, Chemical Sciences Div., University of California, Berkeley, Berkeley, CA 94720

A molecular-thermodynamic model is developed for salt-induced protein precipitation, which considers an aqueous solution of globular protein molecules as a pseudo-one-component system containing macroions that interact through Coulombic repulsion, dispersion attraction and hydrophobic interactions, and forces arising from ion-excluded volume. Forces from ion-excluded volume take into account formation of ion pairs and ionic clusters at high salt concentrations; they are calculated in the context of the Percus–Yevick integral-equation theory. Hydrophobic interactions between exposed nonpolar amino-acid residues on the surfaces of the protein molecules are modeled as short-range, attractive interactions between "spherical caps" on the surfaces of the protein polyions. An equation of state is derived using perturbation theory. From this equation of state we calculate liquid–liquid equilibria: equilibrium between an aqueous phase dilute in protein and another aqueous phase rich in protein, which represents "precipitated" protein. In the equation of state, center-to-center, spherically symmetric macroion–macroion interactions are described by the random-phase approximation, while the orientation-dependent short-range hydrophobic interaction is incorporated through the perturbation theory of associating fluids. The results suggest that either ion-excluded-volume or hydrophobic-bonding effects can precipitate proteins in aqueous solutions with high salt concentrations.

Introduction

In research laboratories and in the biotechnology industry, precipitation is commonly used to separate and isolate proteins from solutions. This technique has been applied to the recovery of proteins such as insulin, diagnostic and industrial enzymes, human growth hormone, and interferon (McGregor, 1983). Separation is achieved through addition of precipitating agents such as inorganic salts at high concentrations, nonionic polymers, polyelectrolytes, and organic solvents. (See, for example, Foster et al., 1973; Haire et al., 1984; Shih et al., 1992; Niederauer and Glatz, 1992; Rothstein, 1994.)

In most previous studies, protein precipitation in concentrated salt solutions has been understood as phase separation resulting in a solid phase (that is, the protein precipitate) and a saturated protein liquid phase. Traditionally, quantitative characterization has been expressed through the protein solubility, that is, the protein concentration in the equilibrium liquid phase. Experimental data indicate that, at fixed temperature, the concentration of protein in the liquid phase is a function of protein size and concentration, electrolyte concentration and type, pH of the solution (that is, net charge on the protein), and interactions between exposed hydrophobic residues on the surface of the protein (Arakawa and Timasheff, 1982, 1984).

However, recent experimental results (Shih et al., 1992) on bovine serum albumin and α-chymotrypsin suggest that salt-induced protein precipitation may be more appropriately viewed as phase separation resulting in two fluid phases: a light (supernatant) fluid phase lean in protein, in equilibrium with a dense (precipitate) fluid phase rich in protein but also containing appreciable amounts of water and salt. According to this view, the degree of separation is appropriately characterized not by the protein concentration in the light phase but by the distribution coefficient, K_e, which is defined as

Present address of Y. C. Chiew: Dept. of Chemical and Biochemical Engineering, Rutgers University, Piscataway, NJ 08855.

the ratio of the protein concentration in the dense precipitate phase to that in the light supernatant phase.

To establish a rational basis for designing a protein-precipitation process, it is useful to develop a model to provide a theoretical framework for interpretation and correlation of protein-precipitation data. The apparent solubility of a protein has been successfully correlated by the Cohn equation, which gives a simple relation between the protein concentration in the light phase and electrolyte ionic strength (Melander and Horvath, 1977; Arakawa and Timasheff, 1984). Melander and Horvath showed that the functional form of the Cohn equation may be interpreted on the basis of solvophobic effects. Recent theoretical studies have been directed at developing more fundamental models that account for the diverse interactions between the constituents in the protein solution on a molecular level. For example, Mahadevan and Hall (1990, 1992) presented a model, based on Barker-Henderson perturbation theory, for protein precipitation by a nonionic polymer. Vlachy et al. (1993) describe a model for liquid–liquid phase separation for solutions of colloids and globular proteins, based on the random-phase approximation. However, these recent theoretical studies are concerned with aqueous solutions where the electrolyte concentration is less than 0.1 molar. Experimental studies clearly show that protein precipitation by salts requires electrolyte concentration in the range 1–10 molar.

This work presents a molecular-thermodynamic model for protein precipitation by inorganic salts. Particular attention is given to highly concentrated salt solutions. The procedure employed here represents the ternary solution (protein, electrolyte, and water) as a pseudo-one-component system containing only a continuous solvent and globular protein molecules. The solvent is an aqueous salt solution. The effect of the solvent on protein–protein interactions is taken into account through the strong influence that it exerts on the following protein–protein interactions: Coulombic (charge–charge) repulsion, dispersion attraction, ion-excluded-volume (or osmotic) attraction, and interactions between exposed hydrophobic groups on the surfaces of two or more protein molecules. Despite its simplicity, the one-component representation has been successful in explaining some experimental properties of colloidal dispersions (Grimson, 1983) and globular-protein solutions (Vlachy et al., 1993). A powerful advantage of this representation is that final results are given by analytical equations based on statistical-mechanical theories.

Derivations of effective two-body potentials are discussed, as well as a derivation of the molecular-thermodynamic equation-of-state model for protein solutions based on the random-phase approximation and the perturbation theory of association. Some results of model calculations are also given.

Protein–Protein Interaction Potentials

In the one-component model, aqueous solutions of globular proteins are represented by an assembly of spherical macroions that interact via effective solvent-dependent potentials. The potential of mean force, $W(r)$, between protein molecules (with diameter d_p and net charge z_p) is given by the sum of five potentials:

$$W(r) = W_{hs}(r) + W_{elec}(r) + W_{disp}(r) + W_{ex}(r) + W_{hy}(r,\omega), \quad (1)$$

where r is the center-to-center distance. Here, $W_{hs}(r)$ is the hard-sphere potential, $W_{elec}(r)$ is the screened Coulombic potential due to electrostatic repulsion, $W_{disp}(r)$ is the attractive dispersion potential, and $W_{ex}(r)$ is the potential due to excluded-volume effects. These four terms are spherically symmetric center-to-center potentials. Also, $W_{hy}(r,\omega)$ represents the interactions between exposed hydrophobic groups on the surfaces of the proteins; this potential depends not only on r but also on molecular relative orientation, indicated by ω.

Hard-sphere and Coulombic repulsions between proteins are represented by

$$W_{hs}(r) = \infty \qquad r \le d_p \quad (2a)$$

$$= 0 \qquad r > d_p, \quad (2b)$$

$$\frac{W_{elec}(r)}{kT} = B\frac{\exp(-\kappa r)}{r} \qquad r > d_p, \quad (2c)$$

where $B = z_p^2 L_B \exp(\kappa d_p)/(1+\kappa d_p/2)^2$ and Bjerrum length $L_B = \beta e^2/4\pi\epsilon_0\epsilon_r$. In Eq. 2c, $z_p e$ is the charge on the polyion, $\beta = 1/kT$, k denotes Boltzmann's constant, $\epsilon_0\epsilon_r$ represents the dielectric permittivity of the solvent, and κ^{-1} is the Debye screening length, where $\kappa^2 = 8\pi L_B N_A I$ and ionic strength $I = 05(z_{an}^2 \rho_{an} + z_{cat}^2 \rho_{cat})$; N_A is Avogadro's number, and z_{an} and z_{cat} are the anion and cation valences, respectively; and ρ_{an} and ρ_{cat} are the ionic number densities.

The attractive dispersion interaction $W_{disp}(r)$ is given by the following expression (Verwey and Overbeek, 1948):

$$W_{disp}(r) = -\frac{H}{12}\left\{\frac{d_p^2}{r^2-d_p^2} + \frac{d_p^2}{r^2} + 2 \ln\left(1-\frac{d_p^2}{r^2}\right)\right\} \quad \text{for } r > d_p, \quad (3)$$

where H represents the Hamaker constant. For large values of r, Eq. 3 reduces to

$$W_{disp}(r) = -\frac{H}{36}\left(\frac{d_p}{r}\right)^6 \quad \text{for } r \gg d_p. \quad (4)$$

Equation 4 is the large-r limit for $W_{disp}(r)$. Although this highly simplified form represents a classical approach to quantifying dispersion interactions, it has been used successfully in modeling phase separation of colloidal systems (Grimson, 1983). We recognize that, as r approaches d_p, Eq. 4 underestimates the contribution of dispersion forces to the total potential of mean force. However, dispersion attraction plays a minor role in protein phase separation in concentrated electrolyte solutions in this model (the underestimation is small compared to the contributions of the other potentials). Therefore, Eq. 4 is used because it provides an analytic equation of state for calculating phase equilibria.

It should be noted that this form of the dispersion potential has no explicit dependence on ionic strength. Any effect of ionic strength on dispersion attraction is assumed to be

very small (Israelachvili and Adams, 1978) and contained within the effective Hamaker constant, which is essentially an adjustable model parameter. Furthermore, since H is primarily a function of particle density (Israelachvili, 1985), it is expected that most proteins have similar values of H since most have roughly the same density (Nir, 1976). In all calculations of protein–protein phase equilibrium based on this model, the chosen values of H correspond to those regressed by Haynes et al. (1991) from membrane osmometry experimental data for α-chymotrypsin in solutions of 0.1 molar ionic strength. Their values for H varied between 5 and 20 kT, depending on solution conditions. In more recent work by Coen et al. (1994), values of the effective Hamaker constant regressed from low-angle-laser-light-scattering data for α-chymotrypsin in solutions of potassium sulfate with ionic strength greater than 1.0 molar appear to be essentially constant at 10 kT.

Ion-excluded-volume potential

The term $W_{ex}(r)$ in Eq. 1 accounts for the attractive interaction between a pair of protein macroions due to the excluded volume of simple electrolyte ions in solution. The literature has reported experimental and theoretical studies of the effect of volume exclusion by solvent or small solutes on macromolecular interactions (Israelachvili, 1985; Henderson and Lozada-Cassou, 1986; Henderson, 1988). Henderson and coworkers computed the potentials of mean force for two large rigid hard spheres immersed in a one-component hard-sphere fluid (Henderson and Lozada-Cassou, 1986; Henderson, 1988) and the adhesive hard-sphere fluid (Jamnik et al., 1991), in the context of the Percus–Yevick (PY) integral-equation theory. Their results reveal that the PY theory provides semiquantitative description of experimental results (Henderson, 1992).

For concentrated salt systems typically used in protein precipitation, ion pairs and larger ionic clusters are expected to form in the electrolyte solution (Robinson and Stokes, 1959). Cluster formation enhances the ion-excluded-volume effect because a cluster is appreciably larger than a single ion, increasing the effective range of the osmotic attraction. The ion-excluded-volume potential of mean force, $W_{ex}(r)$, can be obtained from the radial distribution function $g_{33}(r)$ between two protein particles (denoted by subscript 3), separated by a center-to-center distance r, in an electrolyte solution (electrolyte ions denoted by subscripts 1 and 2). In a system with a single added salt species, all three solute components—cation, anion, and protein—are considered to be simple hard spheres of known diameters immersed in a continuum solvent (water). The interactions between like-charge ions follow the simple hard-sphere potential. Interactions between unlike-charge ions are described by the adhesive hard-sphere (AHS) potential (Baxter, 1968b), which is able to model the formation of ion pairs and higher clusters in the electrolyte solution. In this simple model for ion-excluded-volume effects, it is assumed that the electrostatic interactions between ions are adequately taken into account through the screened Coulombic potential, $W_{elec}(r)$, given in Eq 2c. The ion-excluded-volume potential of mean force $W_{ex}(r)$ acting between two protein molecules can be calculated from the protein–protein radial distribution function $g_{33}(r)$ from the following equation (McQuarrie, 1975):

$$W_{ex}(r,\rho_1,\rho_2) = -kT\ln[g_{33}(r,\rho_1,\rho_2)] = -kT\ln[h_{33}(r,\rho_1,\rho_2)+1] \quad (5)$$

where $h_{33}(r)$ is the total correlation function in the limit $\rho_3 = 0$, and ρ_i is the number density of component i.

To obtain $W_{ex}(r)$, we consider the three-component system that consists of species 1 (ion), 2 (ion), and 3 (protein). The function $g_{33}(r)$ is obtained by solving the set of multicomponent Ornstein–Zernike (OZ) integral equations

$$h_{ij}(r) = c_{ij}(r) + \sum_k \rho_k \int c_{ik}(s)h_{kj}(r-s)\ ds \quad (6)$$

for finite values of ρ_1 and ρ_2 and in the limit $\rho_3 = 0$. Here $h_{ij}(r)$ and $c_{ij}(r)$ are the total correlation function and the direct correlation function of the ij pair. To obtain a solution, we use the Percus–Yevick (PY) approximation. For the adhesive hard-sphere system considered here, the PY theory provides the following boundary conditions:

$$h_{ij}(r) = -1 + \frac{\lambda_{ij}d_{ij}}{12}\delta(r-d_{ij}) \quad 0 < r < d_{ij} \quad (7)$$

$$c_{ij}(r) = 0 \quad r > d_{ij} \text{ (for all } ij \text{ pairs)} \quad (8)$$

where $d_{ij} = (d_i + d_j)/2$, d_i is the diameter of component i, and $\lambda_{ij} = 0$ for $ij \neq 12$ or 21. Due to symmetry, $\lambda_{12} = \lambda_{21}$. Equation 7 implies that the 1–1, 2–2, 3–3, 1–3, and 2–3 interactions are determined by hard-sphere potentials. Clustering between ionic species 1 and 2 is explicitly accounted for by the Dirac delta function $\delta(r-d_{12})$, which is defined so that $\int_0^\infty f(r)\delta(r-d_{12})\ dr = f(d_{12})$. Parameter λ_{12} takes into account the average number of 1–2 direct contacts that are formed in the system; it is related to N_{12}, the average number of species-2 ions that have direct bonds with a species-1 ion by

$$N_{12} = 4\pi\rho_2\int_0^{d_{12}} r^2 g_{12}(r)\ dr = 2\eta_2\lambda_{12}\left(\frac{d_{12}}{d_2}\right)^3, \quad (9)$$

where $\eta_2 = \pi\rho_2 d_2^3/6$. When $N_{12} = 0$, there is no ion clustering. When $N_{12} = 1$, each species-1 ion, on the average, has one species-2 bonded neighbor. When $N_{12} = 2$, each species-1 ion, on the average, has two species-2 bonded neighbors. When the electrolyte is a symmetric salt, $N_{21} = N_{12}$. However, for asymmetric electrolytes, $N_{12} = N_{21}|(z_2/z_1)|$, where z_1 and z_2 are the ion valences.

Because of the short-range nature of $c_{ij}(r)$, the OZ equation can be solved through the use of the Wiener–Hopf factorization technique (Baxter, 1968a). The resulting equation for the protein–protein total correlation function $h_{33}(r)$ is decoupled from the total correlation function $c_{33}(r)$, and can be shown to follow the equation below (Perram and Smith, 1977; Barboy and Tenne, 1979; Chiew, 1991):

$$rh_{33}(r) = \frac{d}{dr}q_{33}(r) + 2\pi\sum_{k=1}^{2}\rho_k\int_{S_{3k}}^{d_{3k}} q_{3k}(t)(r-t)h_{k3}(r-t)\ dt, \quad (10)$$

where $S_{ij} = (d_{ii} - d_{jj})/2$. The functions $h_{13}(r)$ and $h_{23}(r)$ represent the protein-ion total correlation functions; they are obtained from

$$rh_{i3}(r) = \frac{d}{dr}q_{i3}(r) + 2\pi \sum_{k=1}^{2} \rho_k \int_{S_{ik}}^{d_{ik}} q_{ik}(t)(r-t)h_{k3}(r-t)\ dt. \tag{11}$$

In the preceding equations, function $q_{ij}(r)$ is given by

$$q_{ij}(r) = \frac{a_i}{2}\left(r^2 - d_{ij}^2\right) + b_i(r - d_{ij}) + \frac{\lambda_{ij} d_{ij}^2}{12} \quad \text{for } S_{ij} < r < d_{ij} \tag{12a}$$

$$= 0 \qquad \text{for } r > d_{ij} \tag{12b}$$

and

$$\frac{d}{dr}q_{ij}(r) = a_i r + b_i \qquad \text{for } S_{ij} < r < d_{ij} \tag{13a}$$

$$= 0 \qquad \text{for } r > d_{ij}, \tag{13b}$$

where $\lambda_{ij} = 0$ for $ij \neq 12$ or 21. The PY solution provides the following expressions for parameters a_i and b_i (for $i = 1$, 2, and 3):

$$a_i = \frac{1 - H + 3d_{ii}G}{(1-H)^2} - \frac{Y_1}{(1-H)}\delta_{i1} - \frac{Y_2}{(1-H)}\delta_{i2} \tag{14a}$$

$$b_i = -\frac{3d_{ii}^2 G}{2(1-H)^2} + \frac{d_{ii}Y_1}{2(1-H)}\delta_{i1} + \frac{d_{ii}Y_2}{2(1-H)}\delta_{i2} \tag{14b}$$

$$Y_1 = \eta_2 \lambda_{12}\left(\frac{d_{12}}{d_2}\right)^2 \tag{14c}$$

$$Y_2 = \eta_1 \lambda_{12}\left(\frac{d_{12}}{d_1}\right)^2 \tag{14d}$$

$$G = \frac{\pi}{6}\sum_{k=1}^{2} \rho_k d_{kk}^2 \tag{14e}$$

$$H = \frac{\pi}{6}\sum_{k=1}^{2} \rho_k d_{kk}^3 \tag{14f}$$

and the inequality:

$$\frac{1+2H}{(1-H)^2} + \frac{\eta_1\eta_2\lambda_{12}(6-\lambda_{12})}{(1-H)^3} > 0. \tag{14g}$$

Here δ_{ij} is the Kronecker delta, that is, $\delta_{ij} = 1$ for $i = j$, and zero otherwise. The second and third terms on the righthand sides of Eqs. 14a and 14b vanish if $i \neq 1$ and 2, respectively. Equations 12 through 14a–14f are the PY analytic solution of the OZ integral equation, that is, Eq. 6, subject to the boundary conditions given by Eqs. 7 and 8. The PY solution further requires that the inequality given by Eq. 14g must be satisfied to ensure physically admissible solutions (Baxter, 1968; Barboy and Tenne, 1979); this means that λ_{12} or N_{12} depend on the density of the system and must be properly chosen for model calculations. The total correlation function $h_{33}(r)$ is obtained by first calculating $h_{13}(r)$ and $h_{23}(r)$ from Eq. 11, followed by solving $h_{33}(r)$ from Eq. 10; these calculations can be performed using the simple numerical procedure proposed by Perram (1975). That calculation is much simpler than solving the set of multicomponent Ornstein–Zernike integral equations (Eq. 6) simultaneously through a Fourier-transform technique. The potential $W_{ex}(r)$ is related to $h_{33}(r)$ by Eq. 5; it is independent of protein concentration, and depends only on the number densities of ions (species 1 and 2), ion diameters d_1, d_2, and parameter N_{12} that characterizes the degree of ion clustering. Ion number densities ρ_1 and ρ_2 are related by the stoichiometric relation $z_1\rho_1 + z_2\rho_2 = 0$, where z_1 and z_2 are the valences of the ions.

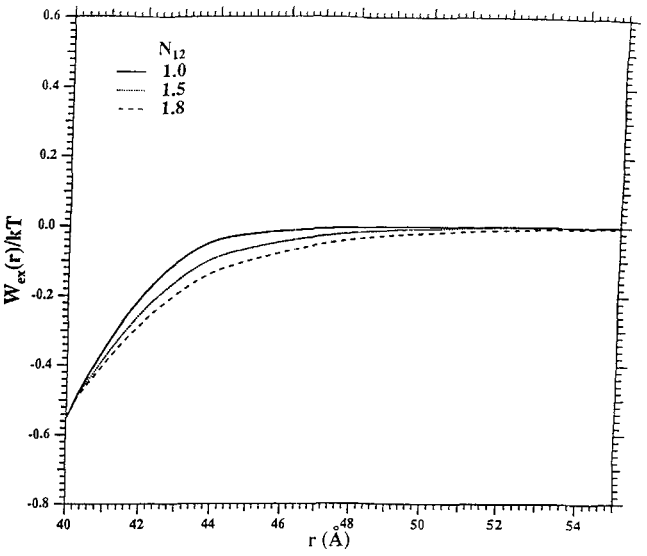

Figure 1. Ion-excluded-volume potential of mean force $W_{ex}(r)/kT$ as a function of protein center-to-center distance for three values of clustering parameter N_{12}.

Other parameters are $d_p = 40$ Å; $d_{an} = 4.6$ Å; $d_{cat} = 2.96$ Å; $|z_{an}| = 2$; $|z_{cat}| = 1$; and salt concentration $C_s = 0.5$ mol/L.

Figure 1 shows the computed potential of mean force $W_{ex}(r)/kT$ plotted as a function of protein–protein center-to-center distance r for different values of N_{12} in a 0.5-M salt solution containing ions with diameters $d_1 = 4.6$ Å and $d_2 = 2.96$ Å, $|z_1| = 2$, $|z_2| = 1$, corresponding to ammonium sulfate. In this figure d_p is taken as 40 Å, roughly equal to the unhydrated diameter of α-chymotrypsin. Potential $W_{ex}(r)/kT$ is attractive and the range of the potential increases with N_{12}, the degree of ionic clustering. Figure 1 indicates that at high salt concentrations, when ionic pairs and clusters are formed, the interaction between protein macroions becomes increasingly attractive. The aqueous electrolyte literature provides guidance in choosing physically reasonable values of N_{12} (Robinson and Stokes, 1959).

In this approximate method of calculating the effect of ion-excluded volume on protein–protein interactions, the electrolyte ions are treated as hard spheres with finite diameter. Assigning a size to the ions is necessary to quantify osmotic attraction in the manner described previously. However, we have also assumed that the Coulombic interactions

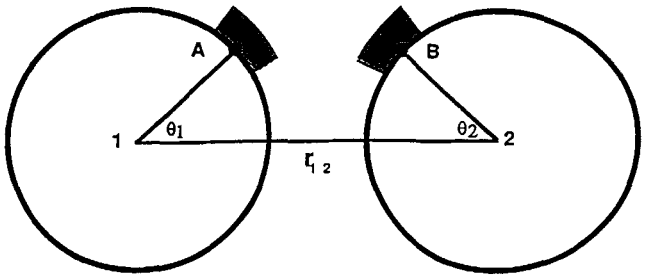

Figure 2. The short-range orientation-dependent hydrophobic interaction.

in the system are adequately described by the well-known Debye–Hückel expression, given in Eq. 2c, which is derived with the assumption that the electrolyte ions are point charges. This assumption is acceptable for calculating Coulombic interactions in low ionic strength solutions, where the characteristic length scale of Coulombic interactions is much greater than that of excluded-volume effects. In systems of high ionic strength, where the magnitude of the Debye length κ^{-1} is similar to the diameter of an electrolyte ion, this assumption is no longer valid. (In practice, however, as proteins approach contact, the discrete nature of their surface charge distribution gives rise to short-range electrostatic interactions that cannot be accurately described by the simple Debye–Hückel expression. Other techniques are being considered to quantify these effects.) However, at these high ionic strengths, the long-range Coulombic interactions are essentially eliminated due to dielectric screening and therefore play a minor role in phase separation. Since it has been observed experimentally that high salt concentrations are typically required to bring about phase separation, we expect that the contribution of ion clustering to the excluded volume interaction $W_{ex}(r)$ plays an important role in the phase separation of proteins in solutions containing concentrated electrolyte. This role is explicitly taken into account through the adhesive hard-sphere model outlined earlier.

Hydrophobic interactions

The hydrophobic interaction between exposed nonpolar amino acid residues on the surfaces of the protein molecules is, in general, attractive, short-range, and orientation-dependent. Hydrophobic bonds are formed when two hydrophobic groups come into contact with each other, and cause association or aggregation of protein molecules in the system. In this work, hydrophobic interaction is represented by a potential model used for associating fluids (Jackson et al., 1988). The shapes of these hydrophobic groups are idealized as "circular patches" or "spherical caps" located on the surface of the macroion. As indicated in Figure 2, interaction potential $W_{hy}(\boldsymbol{r}_{12})$ between hydrophobic "patch" A on the surface of particle 1 and hydrophobic "patch" B on the surface of particle 2 is defined such that

$$W_{hy}(\boldsymbol{r}_{12}) = -\epsilon \text{ if } |r_{12}| \le r_{12,c} \quad \text{and} \quad \boldsymbol{d}_{1,A}\cdot\boldsymbol{r}_{12} \le \cos\theta_{1,c} \quad \text{and} \quad -\boldsymbol{d}_{2,B}\cdot\boldsymbol{r}_{12} \le \cos\theta_{2,c}$$
$$= 0 \text{ otherwise} \qquad (15)$$

where $\boldsymbol{d}_{iK}$ represents the vector joining the center of particle i to the center of patch K (located on the surface of particle i). The quantity $\boldsymbol{r}_{12}$ denotes the vector joining the center of molecule 1 to the center of molecule 2. The vector dot product $\boldsymbol{d}_{1,A}\cdot\boldsymbol{r}_{12} = \cos\theta_1$ where angle θ_1 denotes the angle between $\boldsymbol{r}_{12}$ and $\boldsymbol{d}_{iK}$. Angle θ_2 is defined in a similar manner. Hence, two hydrophobic "patches" on two different particles are considered to form a "bond" if the centers of the two particles are within a distance $r_{12,c}$ from each other, and the two hydrophobic groups satisfy the orientation constraints $\boldsymbol{d}_{1,A}\cdot\boldsymbol{r}_{12} \le \cos\theta_{1,c}$ and $-\boldsymbol{d}_{2,B}\cdot\boldsymbol{r}_{12} \le \cos\theta_{2,c}$. The quantities $r_{12,c}$, $\theta_{1,c}$, and $\theta_{2,c}$ characterize the range of the hydrophobic interaction and the sizes of the hydrophobic groups. In general, these quantities are not known for complex species such as proteins. Fortunately, the thermodynamic properties of systems with this type of interaction can be described in terms of quantities that are known or can be estimated from physicochemical data for proteins, as described below.

Equation of State

Having established and defined pertinent potentials of mean force, it is now necessary to construct a molecular-thermodynamic model that relates these potentials to macroscopic thermodynamic properties. In this work, that model is based on perturbation theory. The center-to-center spherically symmetrical electrostatic, dispersion, and excluded-volume interactions are incorporated into the model in the context of the random-phase approximation. The orientation-dependent hydrophobic interaction is included through the first-order perturbation theory of associating fluids formulated by Wertheim (1986).

The random-phase approximation (RPA) has been used previously to model the phase transition and structure factor of colloids (Grimson, 1983), and to describe liquid–liquid phase separation of proteins due to addition of polymers (Mahadevan and Hall, 1990, 1992; Vlachy et al., 1993). In the RPA, an assembly of hard spheres is used as the reference system, while the remaining spherically symmetric interactions are treated as perturbations. Following Grimson (1983) and Vlachy et al. (1993), the compressibility factor Z_{sym} and residual Helmholtz energy due to spherically symmetric potentials within the RPA are expressed as

$$Z_{sym} = \frac{P}{\rho kT} = Z_{hs} + Z_{pert} = \frac{P_{hs}}{\rho kT} + \frac{\rho U}{2kT} \qquad (16)$$

$$\frac{a^{res}}{kT} = \frac{a^{res}_{hs}}{kT} + \frac{a^{res}_{pert}}{kT} = \frac{a^{res}_{hs}}{kT} + \frac{\rho U}{2kT} \qquad (17)$$

Here P_{hs} and a^{res}_{hs}/kT represent the pressure and residual Helmholtz energy of the hard-sphere reference system, given by the standard Carnahan–Starling expressions (Carnahan-Starling, 1970); ρ is the number density of protein molecules; and U is the perturbation energy per unit density, given by

$$\frac{\rho U}{kT} = \frac{4\pi\rho}{kT}\int [W_{\text{elec}}(r) + W_{\text{disp}}(r) + W_{\text{ex}}(r)]r^2 \quad dr$$

$$= 8\eta z_p^2 L_B \frac{\left[1 + 3/(\kappa d_p) + 3/(\kappa d_p)^2\right]}{d_p(1+\kappa d_p/2)^2} - \frac{4\eta H}{9kT} + \frac{\rho U_{\text{ex}}}{kT} \tag{18}$$

where $U_{\text{ex}} = 4\pi\int W_{\text{ex}}(r)r^2\,dr$ is the contribution to U from the ion-excluded-volume interaction. Because U is an energy per unit density, it is assumed to be independent of protein density; U depends only on potentials of mean force between protein molecules.

The contribution of the non-spherically-symmetric hydrophobic interaction to the residual Helmholtz energy and pressure of the system are evaluated using the first-order perturbation theory of associating fluids formulated by Wertheim (1986, 1987), extended to mixtures by Gubbins and coworkers (Jackson et al., 1988). At a given protein or particle number density ρ and temperature T, this theory gives the Helmholtz energy of the associating system relative to that of the nonassociating reference system. The reference system is an assembly of nonaggregating protein macroions that interact through the spherically symmetric potentials. For a protein molecule consisting of M equivalent exposed hydrophobic sites interacting via the potential given by Eq. 15, the first-order perturbation theory yields the following contribution to the Helmholtz energy due to hydrophobic association (Jackson et al., 1988):

$$\frac{a^{\text{assoc}}}{kT} = M\left[\ln X - \frac{X}{2} + \frac{1}{2}\right]. \tag{19}$$

Here,

$$X = \frac{-1 + \sqrt{1 + 4M\rho\Delta}}{2M\rho\Delta} \tag{20a}$$

$$\Delta = g_{pp}(d_p)[\exp(\epsilon/kT) - 1]V \tag{20b}$$

$$V = 3\frac{[1-\cos(\theta_{1,c})][1-\cos(\theta_{2,c})]}{2\pi}\frac{(r_{12,c} - d_p)}{d_p}, \tag{20c}$$

where M is the number of hydrophobic groups on the protein surface, MX is the fraction of hydrophobic sites that are not bonded, $g_{pp}(d_p)$ is the radial distribution function of the nonaggregating system, and ϵ/kT represents the characteristic energy of the hydrophobic interaction. Dimensionless parameter V corresponds to the volume of interaction between two attractive square-well hydrophobic sites divided by the volume of a single protein particle. The number of sites, M, and the interaction volume, V, can both be estimated by inspection of the protein crystal structure data. It is more difficult to estimate ϵ/kT precisely. For hydrophobic interactions between proteins, a reasonable upper bound is approximately $\epsilon/kT \sim 5$ (Tanford, 1980).

The function $g_{pp}(d_p)$ for the nonagglomerating protein macroions (which interact through the hard-sphere, electrostatic, dispersion, and ion-excluded-volume potentials) is estimated using the EXP approximation (Konior and Jedrzejek, 1985):

$$g_{pp}(d_p) = g_{\text{hs}}(d_p)\cdot\exp\{-[W_{\text{elec}}(d_p) + W_{\text{disp}}(d_p) + W_{\text{ex}}(d_p)]/kT\}, \tag{21}$$

where $g_{\text{hs}}(d_p)$ is given by the contact value of the Carnahan–Starling expression for the hard-sphere radial distribution function:

$$g_{\text{hs}}(d_p) = \frac{1 - \eta/2}{(1-\eta)^3}. \tag{22}$$

The first-order perturbation theory of association assumes that the interactions between hydrophobic sites on different molecules are independent of each other and that no ring structures (only treelike structures) are formed in the protein aggregates. Combining contributions to the residual Helmholtz energy and compressibilty factor from spherically symmetric and nonsymmetric interactions, it follows that Z and a^{res}/kT are given by

$$Z = \frac{P}{\rho kT} = \frac{1 + \eta + \eta^2 - \eta^3}{(1-\eta)^3} + \frac{\rho U}{2kT} + M\left\{\frac{1}{X} - \frac{1}{2}\right\}\eta\left(\frac{\partial X}{\partial \eta}\right)_T \tag{23}$$

and

$$\frac{a^{\text{res}}}{kT} = \frac{4\eta - 3\eta^2}{(1-\eta)^2} + \frac{\rho U}{2kT} + M\left[\ln X - \frac{X}{2} + \frac{1}{2}\right]. \tag{24}$$

Chemical potential μ/kT can be obtained from Eqs. 23 and 24 through the thermodynamic relation $\mu^{\text{res}}/kT = a^{\text{res}}/kT + Z - 1$, and the ideal gas chemical potential, $\mu^{\text{ig}}/kT = \mu^*/kT + \ln\rho$, where μ^* is a function only of temperature. We obtain

$$\frac{\mu - \mu^*}{kT} = \ln\rho + \frac{\eta(8 - 9\eta + 3\eta^2)}{(1-\eta)^3} + \frac{\rho U}{kT} + M\left\{\ln X - \frac{X}{2} + \frac{1}{2} + \eta\left(\frac{\partial X}{\partial \eta}\right)_T\left[\frac{1}{X} - \frac{1}{2}\right]\right\}. \tag{25}$$

Here, $\mu^*/kT = \ln(\Lambda^3)$; the deBroglie wavelength $\Lambda = h/\sqrt{2\pi mkT}$, where h is Planck's constant and m is the molecular mass. Energy per unit density U, given by Eq. 18, gives the effects of electrostatic, dispersion, and ion-excluded-volume interactions. At equilibrium, protein concentrations in the supernatant and dense-fluid phases are calculated from Eqs. 24 and 25 based on the classical equilibrium conditions:

$$\mu_s = \mu_d \tag{26a}$$

$$P_s = P_d. \tag{26b}$$

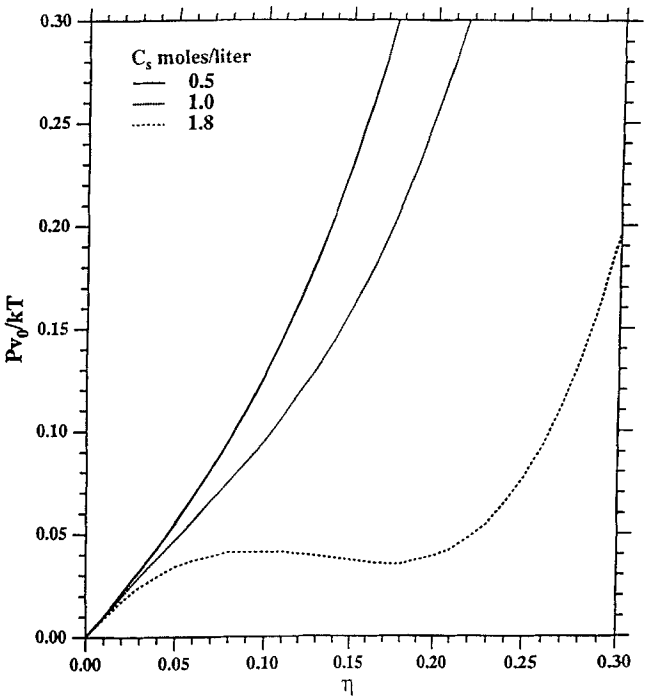

Figure 3. Reduced pressure as a function of protein packing fraction η for three salt concentrations.

Other parameters are $d_p = 40$ Å; $d_{an} = 4.6$ Å; $d_{cat} = 2.96$ Å; $|z_p| = 5$; $|z_{an}| = 2$; $|z_{cat}| = 1$; $H/kT = 9.6$; and $N_{12} = 1$.

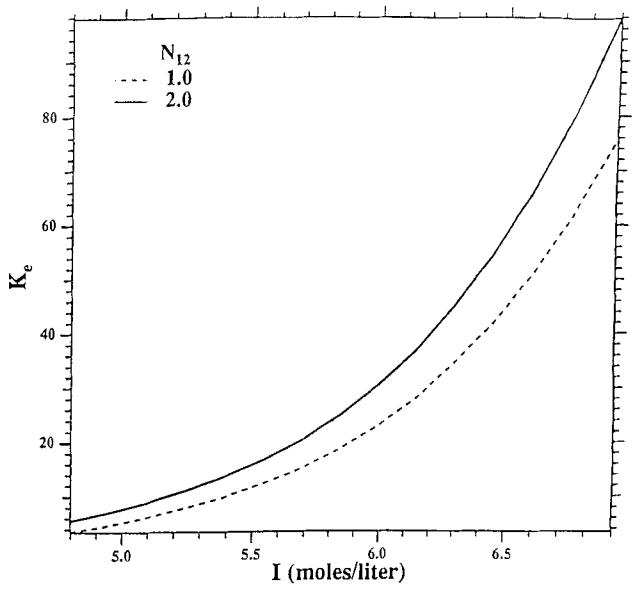

Figure 4. Distribution coefficient K_e as a function of ionic strength I for two values of N_{12}.

Other parameters are $d_p = 40$ Å; $d_{an} = 4.6$ Å; $d_{cat} = 2.96$ Å; $|z_p| = 5$; $|z_{an}| = 2$; $|z_{cat}| = 1$; $H/kT = 9.6$.

Here, subscripts s and d denote the equilibrium supernatant and dense protein phases, respectively. In Eq. 26a, μ^* cancels out.

Results and Discussion

We first examine the effect of salt concentration on the phase behavior of the system. Figure 3 shows the reduced pressure PV_0/kT, computed from Eq. 27, plotted as a function of the protein volume fraction η for the system where $d_p = 40$ Å, $d_{an} = 4.6$ Å, $d_{cat} = 2.96$ Å, $|z_p| = 5$, $|z_{an}| = 2$, $|z_{cat}| = 1$, $H/kT = 9.6$, and $N_{12} = 1$, with different values of salt concentrations C_s, in the absence of hydrophobic interactions. Here V_0 represents the volume of a single protein molecule. The pressure increases monotonically with protein volume fraction η at the two lower salt concentrations. However, when $C_s = 1.8$ mol/L, the pressure curve exhibits a van der Waals loop, indicating that the system undergoes a fluid–fluid phase transition. This result suggests that rising electrolyte concentrations increase the excluded-volume attraction between proteins, leading to phase separation. As in Figure 1, the given salt and protein size parameters correspond to ammonium sulfate and α-chymotrypsin. In all calculations the chosen values of the Hamaker constant corresponded to those regressed from membrane osmometry data by Haynes et al. (1992).

The distribution coefficient K_e of the protein system can be obtained from the equilibrium conditions. The distribution coefficient K_e is given by the ratio of the equilibrium number density of protein in the dense phase to that in the supernatant phase. Neglecting hydrophobic interactions, Figure 4 shows predicted distribution coefficient K_e plotted as a function of ionic strength for systems where $d_p = 40$ Å, $d_{an} = 4.6$ Å, $d_{cat} = 2.96$ Å, $|z_p| = 5$, $|z_{an}| = 2$, $|z_{cat}| = 1$, and $H/kT = 9.6$, for two values of N_{12}. Coefficient K_e increases monotonically with electrolyte concentration. For all calculated phase equilibria, the weight fractions of protein in the supernatant were 1% or less and varied from 10% to 30% in the dense phase. These results are consistent with phase compositions measured by Shih et al. (1992) for salt-induced precipitation of α-chymotrypsin and hen-egg-white lysozyme.

Again neglecting hydrophobic interactions, Figure 5 shows the variation of distribution coefficient K_e as a function of z_p, the net charge of protein, where $d_p = 40$ Å, $d_{an} = 4.6$ Å, $d_{cat} = 2.96$ Å, $|z_{an}| = 2$, $|z_{cat}| = 1$, $H/kT = 8$, corresponding to α-chymotrypsin in $(NH_4)_2SO_4$, with $N_{12} = 1$, and $I = 6.0$ and 6.6 mol/L. Ionic strength has a strong impact on protein precipitation. At a fixed value of z_p, distribution coefficient K_e increases by nearly a factor of 2 as the ionic strength increases from 6.0 to 6.6 mol/L. This increase in K_e is due to the enhanced effect of the ion-excluded-volume contribution. Distribution coefficient K_e is insensitive to z_p because long-range Coulombic repulsion between protein molecules is screened out in highly concentrated salt solutions. Since the protein charge z_p is directly related to the pH of the solution, this prediction further implies that, in our model, pH has little influence on phase separation.

Figure 6 shows experimental values for K_e for α-chymotrypsin in solutions of ammonium sulfate at various ionic strengths (Coen et al., 1994). An increase in K_e is observed as pH moves away from the isoelectric point, the point of zero net charge on the protein (pI = 8.3). Whether this is an electrostatic effect due to short-range asymmetric Coulombic interactions not described by Eq. 2c is currently under investigation. Other possible explanations, such as in-

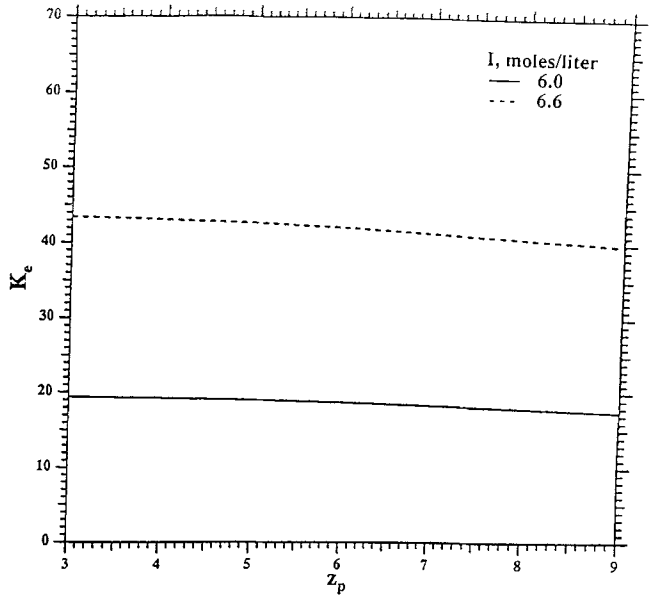

Figure 5. Distribution coefficient K_e as a function of net charge of protein z_p for two ionic strengths.

Other parameters are $d_p = 40$ Å; $d_{an} = 4.6$ Å; $d_{cat} = 2.96$ Å; $|z_{an}| = 2$; $|z_{cat}| = 1$; $H/kT = 8$; and $N_{12} = 1$.

creased counterion binding or protein conformational changes at low pH, may also contribute. Furthermore, comparison of Figures 5 and 6 shows that model calculations overpredict equilibrium phase separation, although semiquantitative agreement with experimental data is achieved.

We now present calculations on the effect of hydrophobic interactions on protein phase separation. The contribution of the hydrophobic interaction to the thermodynamic properties of the system is primarily characterized by M, the number of

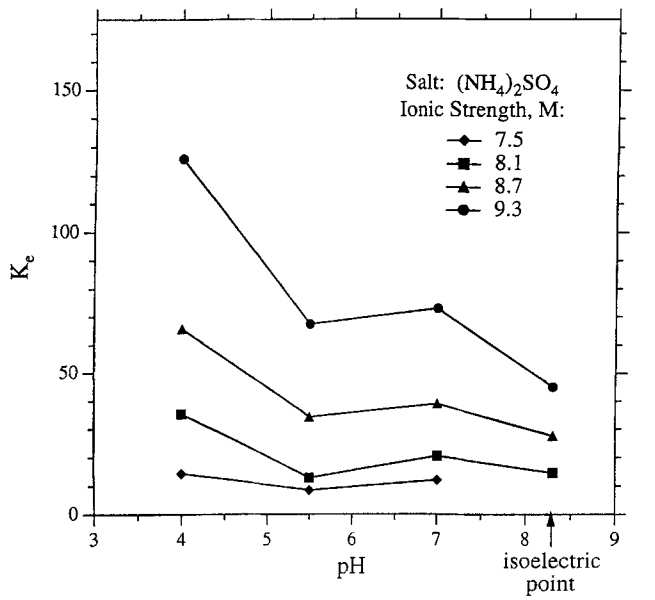

Figure 6. Experimental values of K_e as a function of pH for α-chymotrypsin in solutions of $(NH_4)_2SO_4$. (Data shown with the permission of Coen et al.)

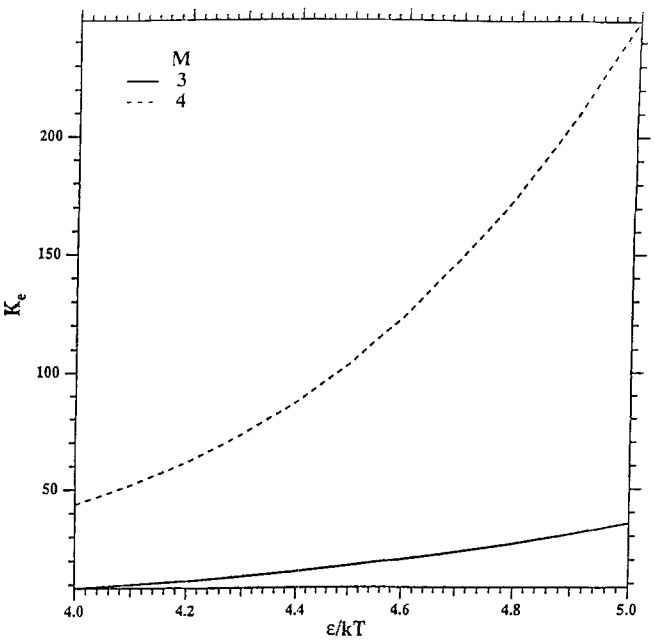

Figure 7. Distribution coefficient K_e as a function of hydrophobic interaction energy ϵ/kT for two values of M.

Other parameters are $d_p = 40$ Å; $d_{an} = d_{cat} = 3.4$ Å; $|z_p| = 8$; $|z_{an}| = 1$; $|z_{cat}| = 1$; $H/kT = 6$; $I = 2.5$ mol/L, $V = 0.006$; and $N_{12} = 1$.

hydrophobic sites, and ϵ/kT and V, the characteristic energy and volume of hydrophobic attraction, respectively. Figure 7 shows distribution coefficient K_e as a function of ϵ/kT, where $d_p = 40$ Å, $d_{an} = d_{cat} = 3.4$ Å, $|z_p| = 8$, $|z_{an}| = 1$, $|z_{cat}| = 1$ (now corresponding to a monovalent electrolyte, such as KCl), $H/kT = 6$, $I = 2.5$ mol/L, $V = 0.006$, and $N_{12} = 1$, for two different values of M. It is apparent from this figure that hydrophobic bonding has a significant impact on phase separation. Higher K_e are obtained at lower ionic strengths through incorporation of hydrophobic effects. Distribution coefficient K_e increases with ϵ/kT because as the strength of hydrophobic attraction rises, protein molecules tend to form aggregates. Aggregation increases the protein concentration in the precipitate phase, and lowers the protein concentration in the supernatant phase. At a fixed ϵ/kT, distribution coefficient K_e increases with M, the average number of exposed hydrophobic sites.

We now examine the effect of Hamaker constant H/kT on the phase separation of proteins. Figure 8 shows distribution coefficient K_e as a function of ionic strength where $d_p = 40$ Å, $d_{an} = d_{cat} = 3.4$ Å, $|z_p| = 8$, $|z_{an}| = 1$, $|z_{cat}| = 1$, $\epsilon/kT = 4$, $M = 4$, $V = 0.006$, and $N_{12} = 1$, for three reduced Hamaker constants, H/kT. Distribution coefficient K_e increases with rising H/kT at fixed I. Figure 9 shows distribution coefficient K_e as a function of protein diameter d_p, where $d_{an} = d_{cat} = 3.4$ Å, $|z_p| = 8$, $|z_{an}| = 1$, $|z_{cat}| = 1$, $H/kT = 6$, $I = 2.5$ mol/L, $\epsilon/kT = 4$, $M = 4$, $V = 0.006$, and $N_{12} = 1$. Distribution coefficient increases with increasing d_p, consistent with experimental observations.

Finally, we study the variation of K_e with ion diameters. For a given electrolyte, accurate values for cation and anion diameters in aqueous solutions may be found in the *literature*

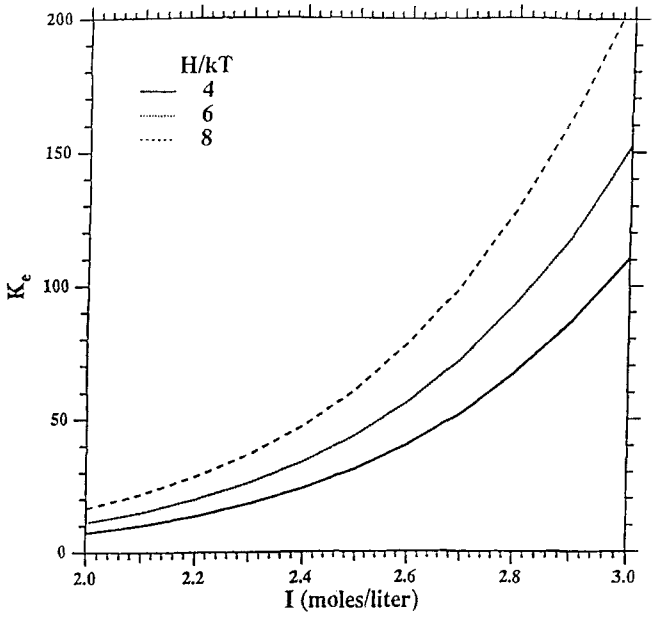

Figure 8. Distribution coefficient K_e as a function of ionic strength I for three values of H/kT.

Other parameters are $d_p = 40$ Å; $d_{an} = d_{cat} = 3.4$ Å; $|z_p| = 8$; $|z_{an}| = 1$; $|z_{cat}| = 1$; $H/kT = 6$; $\epsilon/kT = 4$; $M = 4$; $V = 0.006$; and $N_{12} = 1$.

(Dean, 1985; Burgess, 1978). Figure 10 shows the distribution coefficient K_e as a function of ion diameter for a monovalent electrolyte with $d_{an} = d_{cat} = d_{ion}$, where $|z_{an}| = 1$, $|z_{cat}| = 1$, $d_p = 40$ Å, $|z_p| = 8$, $H/kT = 4$, $\epsilon/kT = 4$, $M = 4$, $V = 0.006$, and $N_{12} = 1$, at two values of I. As expected, K_e increases strongly with increasing ion diameter, especially at high salt concentration. Figure 10 indicates once again the strong dependence of phase separation on ionic strength.

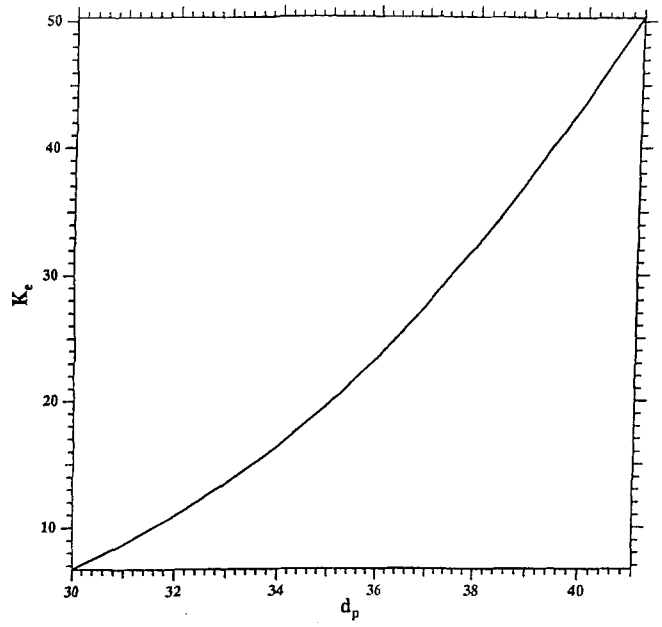

Figure 9. Distribution coefficient K_e as a function of protein diameter d_p.

Other parameters are $d_p = 40$ Å; $d_{an} = d_{cat} = 3.4$ Å; $|z_p| = 8$; $|z_{an}| = 1$; $|z_{cat}| = 1$; $H/kT = 6$; $I = 2.5$ mol/L, $\epsilon/kT = 4$; $M = 4$; $V = 0.006$; and $N_{12} = 1$.

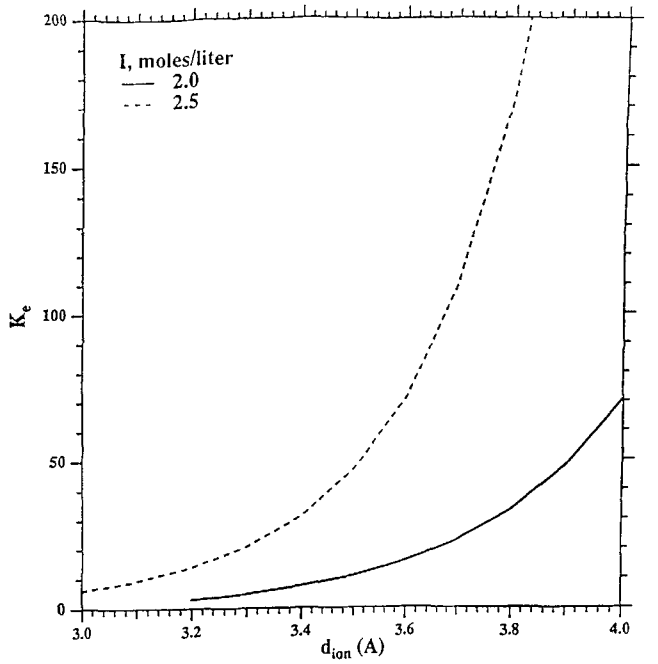

Figure 10. Distribution coefficient K_e as a function of ionic diameter for two ionic strengths.

Other parameters are $d_p = 40$ Å; $d_{an} = d_{cat} = d_{ion}$; $|z_p| = 8$; $|z_{an}| = 1$; $|z_{cat}| = 1$; $H/kT = 4$; $\epsilon/kT = 4$; $M = 4$; $V = 0.006$; and $N_{12} = 1$.

Conclusion

In summary, we have derived an approximate statistical-mechanical equation-of-state model for salt-induced protein precipitation. In this model, proteins are considered to be macroions that interact with electrostatic repulsion, dispersion attraction, ion-excluded-volume attraction, and hydrophobic interactions. Thermodynamic properties of the system are derived using perturbation theory. The model indicates that (1) distribution coefficient K_e is insensitive to net charge of protein due to strong electrostatic screening at high salt concentrations; (2) electrolyte concentration plays a major role in affecting phase separation in protein solutions; distribution coefficient K_e increases monotonically with salt concentration; (3) distribution coefficient K_e is particularly sensitive and rises with ion diameters, protein diameter, and ionic clustering; and (4) aggregation of protein due to hydrophobic interactions may play an important role in the precipitation of proteins at high salt concentrations; the extent of aggregation is a strong function of M, the average number of exposed associating sites. Model calculations of equilibrium phase separation are in semiquantitative agreement with experimental results.

Precipitation of proteins by concentrated electrolyte may result from ion-excluded-volume effects or from hydrophobic-bond aggregation, or both. Using physically reasonable parameters, either excluded volume or aggregation can be used to interpret protein-precipitation data. In this work, we

have considered solutions with high salt concentrations, where ion-excluded-volume effects are dominant. However, because a decrease in temperature can precipitate proteins in solutions with little added electrolyte, it is likely that specific or hydrophobic interactions leading to aggregation are also important. The relative weights of these effects can be estimated only from experimental studies.

Acknowledgments

This work was supported by the National Science Foundation, under grant BCS 9214653, and by the Director, Office of Energy Research, Office of Basic Energy Sciences, Chemical Sciences Division of the U.S. Department of Energy. Y. C. Chiew thanks John Prausnitz for his kind hospitality when Y. C. C. spent his sabbatical leave at the University of California, Berkeley, in fall 1992.

Notation

a = Helmholtz energy, J/mol
e = elementary charge, 1.602×10^{-19} C
$h_{ij}(r)$ = total correlation function of ij pair
ϵ_r = relative permittivity
ϵ_0 = permittivity in vacuum, C/Vm

Literature Cited

Arakawa, T., and S. N. Timasheff, "Preferential Interactions of Proteins with Salts in Concentrated Solutions," *Biochemistry*, **21**, 6545 (1982).

Arakawa, T., and S. N. Timasheff, "Mechanism of Protein Salting-In and Salting-Out by Divalent Cation Salts: Balance Between Hydration and Salt Binding," *Biochemistry*, **23**, 5912 (1984).

Baxter, R. J., "Ornstein-Zernike Relation for a Disordered Fluid," *Aust. J. Phys.*, **21**, 563 (1968).

Baxter, R. J., "Percus-Yevick Equation for Hard Spheres with Surface Adhesion," *J. Chem. Phys.*, **49**, 2770 (1968).

Barboy, B., and R. Tenne, "Distribution Functions and Equations of State of Sticky Hard Sphere Fluids in the Percus-Yevick Approximation," *Chem. Phys.*, **38**, 369 (1979).

Burgess, J., *Metal Ions in Solution*, Halsted Press, New York (1978).

Chiew, Y. C., "Sol-Gel Transition in Dense Dispersions: Effect of Particle Bridging," *J. Coll. Inter. Sci.*, **143**, 397 (1991).

Carnahan, N., and K. Starling, "Thermodynamic Properties of a Rigid-Sphere Fluid," *J. Chem. Phys.*, **53**, 600 (1970).

Coen, C. J., H. W. Blanch, and J. M. Prausnitz, "Salting Out of Aqueous Proteins: Phase Equilibria and Intermolecular Potentials," *AIChE J.*, **41**, 996 (1995).

Dean, J. A., ed., *Lange's Handbook of Chemistry*, 13th ed., McGraw-Hill, New York (1985).

Foster, P. R., P. Dunhill, and M. D. Lilly, "The Precipitation of Enzymes from Cell Extracts of Saccharomyces Cerevisiae by Polyethylene-Glycol," *Biochem. Biophys. Acta*, **317**, 505 (1973).

Grimson, M. J., "Small Angle Scattering from Colloidal Dispersions," *J. Chem. Soc. Faraday Trans. II*, **79**, 817 (1983).

Haire, R. N., W. A. Tisel, J. C. White, and A. Rosenberg, "On the Precipitation of Proteins by Polymers: The Hemoglobulin-Polyethylene Glycol System," *Biopolymers*, **23**, 2761 (1984).

Haynes, C. A., K. Tamura, H. R. Körfer, H. W. Blanch, and J. M. Prausnitz, "Thermodynamic Properties of Aqueous α-Chymotrypsin Solutions from Membrane Osmometry Measurements," *J. Phys. Chem.*., **96**, 905 (1992).

Henderson, D., "An Explicit Expression for the Solvent Contribution to the Force Between Colloidal Particles Using a Hard Sphere Model," *J. Coll. Inter. Sci.*, **121**, 486 (1988).

Henderson, D., and M. Lozada-Cassou, "A Simple Theory for the Force Between Spheres Immersed in a Fluid," *J. Coll. Inter. Sci.*, **114**, 180 (1986).

Henderson, D., "The Interaction Between Macrospheres in Solution," *Fluid Phase Equil.*, **76**, 1 (1992).

Israelachvili, J. N., and G. E. Adams, *J. Chem. Soc. Farad. Trans. I*, **74**, 975 (1978).

Israelachvili, J. N., *Intermolecular and Surfaces Forces*, Academic Press, London/New York (1985).

Jackson, G., W. G. Chapman, and K. E. Gubbins, "Phase Equilibria of Associating Fluids: Spherical Molecules with Multiple Bonding Sites," *Molec. Phys.*, **65**, 1 (1988).

Jamnik, A., D. Bratko, and D. J. Henderson, "Lyophobic Interaction in Baxter's Adhesive Fluid," *J. Chem. Phys.*, **94**, 8210 (1991).

Konior, J., and C. Jedrzejek, "Analytic Formulation of the WCA Type Perturbation Theory for a Hard-Core with One-Yukawa Tail Fluid," *Molec. Phys.*, **55**, 187 (1985).

Mahadevan, H., and C. K. Hall, "Statistical-Mechanical Model of Protein Precipitation by Nonionic Polymer," *AIChE J.*, **36**, 1517 (1990).

Mahadevan, H., and C. K. Hall, "Theory of Precipitation of Protein Mixtures by Nonionic Polymer," *AIChE J.*, **38**, 573 (1992).

McGregor, W. C., "Large Scale Isolation and Purification of Proteins from Recombinant *E. Coli*," *Ann. N. Y. Acad. Sci.*, **413**, 231 (1983).

McQuarrie, D. A., *Statistical Mechanics*, Harper-Collins, New York (1976).

Melander, W., and C. Horvath, "Salt Effect on Hydrophobic Interactions in Precipitation and Chromatography of Proteins: An Interpretation of the Lyotropic Series," *Arch. Biochem. Biophys.*, **183**, 200 (1977).

Niederauer, M. Q., and C. E. Glatz, "Selective Precipitation," *Adv. Biochem. Eng. Technol.*, **47**, 159 (1992).

Nir, S., "Van der Waals Interactions Between Surfaces of Biological Interest," *Prog. Surf. Sci.*, **8**, 1 (1976).

Perram, J. W., "Hard Sphere Correlation Functions in the Percus-Yevick Approximation," *Mol. Phys.*, **30**, 1505 (1975).

Perram, J. W., and E. R. Smith, "Competitive Adsorption via the Percus-Yevick Approximation," *Proc. Roy. Soc. Lond.*, **A353**, p. 193 (1977).

Robinson, R. A., and R. H. Stokes, *Electrolyte Solutions*, Academic Press, New York (1959).

Rothstein, F., "Differential Precipitation of Proteins," in *Protein Purification Process Engineering*, R. G. Harrison, ed., Marcel Dekker, New York, p. 115 (1994).

Shih, Y.-C., J. M. Prausnitz, and H. W. Blanch, "Some Characteristics of Protein Precipitation by Salts," *Biotech. Bioeng.*, **40**, 1155 (1992).

Tanford, C., *The Hydrophobic Effect: Formation of Micelles and Biological Membranes*, 2nd ed., Wiley, New York (1980).

Verwey, E. J. W., and J. Th. G. Overbeek, *Theory of the Stability of Lyophobic Colloids*, Elsevier, New York (1948).

Vlachy, V., H. W. Blanch, and J. M. Prausnitz, "Liquid-Liquid Phase Separations in Aqueous Solutions of Globular Proteins," *AIChE J.*, **39**, 215 (1993).

Wertheim, M. S., "Fluids with Highly Directional Attractive Forces. III. Multiple Attraction Sites," *J. Stat. Phys.*, **42**, 459 (1986).

Wertheim, M. S., "Fluids with Highly Directional Attractive Forces. IV. Equilibrium Polymerization," *J. Stat. Phys.*, **42**, 477 (1986).

Manuscript received May 9, 1994, and revision received Nov. 7, 1994.